Thermoplasmonic shift and dispersion in thin metal films

A. L. Lereu[a)]
Oak Ridge National Laboratory, Oak Ridge, Tennessee 37831 and Institut de Ciències Fotòniques (ICFO), 08860 Castelldefels (Barcelona), Spain

A. Passian[b)]
Oak Ridge National Laboratory, Oak Ridge, Tennessee 37831 and Department of Physics and Astronomy, University of Tennessee, Knoxville, Tennessee 37996

R. H. Farahi
Oak Ridge National Laboratory, Oak Ridge, Tennessee 37831

N. F. van Hulst
Institut de Ciències Fotòniques (ICFO), 08860 Castelldefels (Barcelona), Spain and Institució Catalana de Recerca i Estudis Avançats (ICREA), 08015 Barcelona, Spain

T. L. Ferrell
Department of Physics and Astronomy, University of Tennessee, Knoxville, Tennessee 37996

T. Thundat
Oak Ridge National Laboratory, Oak Ridge, Tennessee 37831 and Department of Physics and Astronomy, University of Tennessee, Knoxville, Tennessee 37996

(Received 2 October 2007; accepted 25 February 2008; published 1 July 2008)

In 2004, the authors reported two coupling schemes based on the thermo-optic properties of thin metallic films and their associated sub- and superstrates, by utilizing surface plasmons. These studies showed a potential for all-optical modulation at low rates that may be used for sensing purposes. In this article, they continue by investigating thermal processes involved in thin metallic films with different approaches. They first experimentally imaged the shift of the surface plasmon dispersion relation in the visible spectrum, as the thin film temperature is externally varied. They then reinforce the previous observations by collecting the absorption curves at selected visible photon energies of excitation, as the film temperature in the excitation region increases. Utilizing the absorption measurements, they briefly address how one may obtain the real and imaginary parts of the index of refraction of the thin film as a function of temperature for each involved wavelength. Finally, they investigate the local physical state of the film by optically profiling the surface plasmon excitation region. © *2008 American Vacuum Society.* [DOI: 10.1116/1.2900713]

I. INTRODUCTION

Thermal effects, encountered in thin metal films and nanostructures, induce changes in a number of parameters of the material that may be summarized by the variations of quantities such as the thermal expansion coefficient and the thermo-optic coefficient. The thermal expansion coefficient depends on the density of the material, whereas the thermo-optic coefficient takes into account the optical properties, as it represents the variation of the index of refraction n as a function of temperature T. In our study, we attempt to investigate the response of the thin film as well as the variation of n, employing the surface plasmon (SP) dispersion relation, which for a simple dielectric-metal interface takes the form $\kappa=\sqrt{\epsilon_1\epsilon_2/(\epsilon_1+\epsilon_2)}$, where $\epsilon_1=n_1^2$ and $\epsilon_2(\omega)=n_2^2$ are the dielectric functions of the dielectric and metallic media, respectively. Temperature variations have been considered in numerous studies, including those in the context of scanning tunneling microscopy[1,2] and in metallurgical operations.[3] Surface plasmons[4] have been utilized in many applications by the means of their extraordinary optical properties, such as surface characterization and imaging,[5,6] or sensors.[7,8] SPs were first used in estimating surface temperature in 1990 by Herminghaus and Leiderer.[9] These measurements led, thereafter, to experimentally[10,11] and theoretically[12] explore optical temperature sensors based on SPs. Chiang *et al.*[13] have numerically investigated the high temperature effect in the SP resonance (SPR) sensors.

More recently, we reported thermally mediated couplings between multiple SPs,[14–16] or between a current and SPs,[15,17] as a tool for optical modulation. Several beams of different photons energies were shown to be modulated via the excitation of SPs and their mutual thermally induced couplings. In these interactions, thermal processes play an important role, and the frequency f dependence of modulation was experimentally shown to follow a $1/f$ behavior fairly well, and that the highest achieved frequency of modulation did not exceed 10 kHz. In this article, we prospect thermal aspects influencing the SP resonance conditions, by modifying the thin metal film temperature, which may intervene in the couplings presented in our previous works.[14–18] In Sec. II, we first record the shift in the SP dispersion relation, in the vis-

[a)]Present address: Institut Fresnel, CNRS 6133, Campus St. Jérôme, 13397 Marseille, France.
[b)]Electronic mail: passianan@ornl.gov

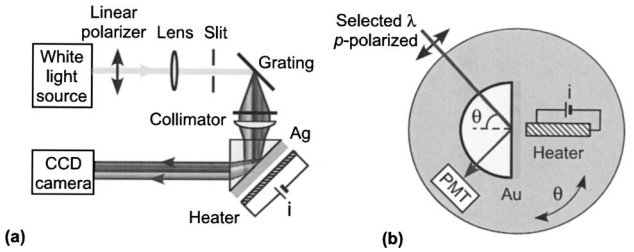

FIG. 1. Experimental arrangements. In (a), a collimated white source excites SPs in the visible range. The light source is p polarized and is guided through a grating to disperse into the visible spectrum before reaching a 40 nm silver film via a right-angled prism in the Kretschmann configuration. An external heater, brought close to the film (within 0.3 mm), is used to increase the film temperature and perturbate the SP resonance conditions. A CCD camera is used to record the changes in the reflected spectrum. In (b), a 55 nm gold film, vacuum deposited onto a hemicylindrical prism, is used to excite SPs for selected wavelengths. The prism-heater assembly is mounted on a computer controlled rotation stage, and the reflectance measurements are carried out with a PMT connected to a computer data acquisition system. In this case, only the SP region is heated.

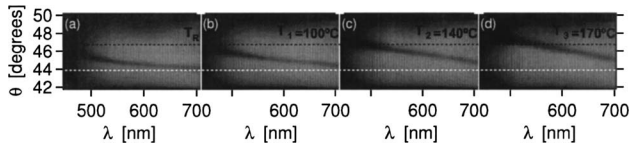

FIG. 2. Highlight of the SP excitation in a 40 nm thin silver film, in the visible spectrum, while the film is externally heated [see Fig. 1(a)]. In (a), the dark line shows the SP excitation at room temperature T_R. (b) is obtained for a film temperature increased to $T_1=100\ ^\circ\mathrm{C}$. (c) and (d) are taken for higher temperatures of $T_2=140\ ^\circ\mathrm{C}$ and $T_3=170\ ^\circ\mathrm{C}$, respectively. A large shift in the dispersion relation is observed as the film temperature is raised from T_R (a) to T_3 (d).

ible range, as the film temperature externally increased. The SP dispersion relation was first imaged in 1985 by Ferrell *et al.*,[5] at room temperature, by using the Kretschmann configuration,[19] and later in 1996 by Kitson *et al.*,[20] while they were exploring the band gap of the SPs on a corrugated surface. Yoon *et al.*[21] highlighted the same measurements by using gratings, as a support for the SP excitation. In Sec. II, we also present measurements of the absorption curves that may be used to access the real (n) and imaginary (k) parts of the index of refraction of the thin film, as a function of its temperature, at selected visible wavelengths. Finally, in Sec. III, we report the optical profile of the SP excitation region from the superstrate (external side of the film) in the aim of studying the film properties under the SP conditions. For analogy, this experimental arrangement presents the capability for optical modulation with similar behavior as reported in Refs. 14–18. A conclusion ends the paper in Sec. IV.

II. TEMPERATURE INFLUENCE ON THE SP RESONANCE CONDITIONS

A. SP dispersion relation

Schemes of the experimental arrangements, displaying the Kretschmann configuration and the optical excitation path, are given in Fig. 1. In the setup described in Fig. 1(a), a beam from a white light source (150 W xenon lamp) passes through a linear polarizer for p polarization, a slit, and is then dispersed via a grating. A collimation and focusing stage is used to create a well-defined excitation beam that can be focused onto a 40 nm silver film supported by a right-angled prism. By using vacuum evaporation, all the metal films, throughout this work, were directly deposited onto the prism without the use of an adhesion layer. A strong advantage of this arrangement is that the film may be excited at different angles at the same time with no moving parts and no change in excitation location.[5] The thickness of the silver film is chosen to be 40 nm to visualize the reflected beam in a range of wavelengths from 450 to 700 nm. A charged coupled device (CCD) camera is utilized to record the reflected beam comprised of a simultaneous range of wavelengths and angles. The CCD is only optimized for wavelengths from 450 nm to near infrared (1.1 μm). A resistive heater designed for this experiment is then mechanically brought close to the film (within 0.3 mm) to increase its temperature, as shown in Fig. 1(a). The resulting images, depicted in Figs. 2(a)–2(d), show a shift of the energy loss from the excited photons to the SPs, in the direction of the higher angles at lower wavelengths, accompanied with a slight widening as the temperature of the film increases. In Fig. 2, the temperature is raised from room temperature T_R [Fig. 2(a)] to $T_1=100\ ^\circ\mathrm{C}$ in Fig. 2(b), then to $T_2=140\ ^\circ\mathrm{C}$ in Fig. 2(c), and finally up to $T_3=170\ ^\circ\mathrm{C}$ in Fig. 2(d). As it can be observed, the higher the temperature is, the larger the angular shift of the SP dispersion relation is. A comparison with the experimental dispersion relation, by using the same silver film parameters as the experiment, is carried out in Fig. 3 for T_R. The simulation is in good agreement with the experimental results, showing, for example, for a wavelength of 700 nm a measured angle of 44.4° for a calculated angle of 44.7° (see the caption of Fig. 3). The simulations were carried out by using the dielectric function of silver compiled by Palik.[22] A larger difference is observed for the smaller wavelengths but stays below 1°. This may be explained by the broadening of the dispersion curve for smaller wavelengths. Also noteworthy is that for temperatures below T_1, the resolution of the system does not permit the distinguishment of either the shift or the broadening of the dispersion relation.

B. Reflectance measurements

For the second arrangement, described in Fig. 1(b), selected wavelengths, in a range of 440–700 nm, are used to excite SPs in a 55 nm gold film via a hemicylindrical quartz prism. A controlled rotation stage varies the incident angle from 40° to 70° with an increment of 0.1°, and a photomultiplier tube (PMT) measures the intensity of the corresponding reflected beam. Thus, we are able to obtain the absorption curves for each wavelength (λ=442, 514, 575, 600, 625, and 650 nm), as depicted in Fig. 4. The temperature of the illuminated region of the gold film is then locally increased from room temperature T_R to $T_a=65\ ^\circ\mathrm{C}$, and then to $T_b=100\ ^\circ\mathrm{C}$. The same data measurements and processing are

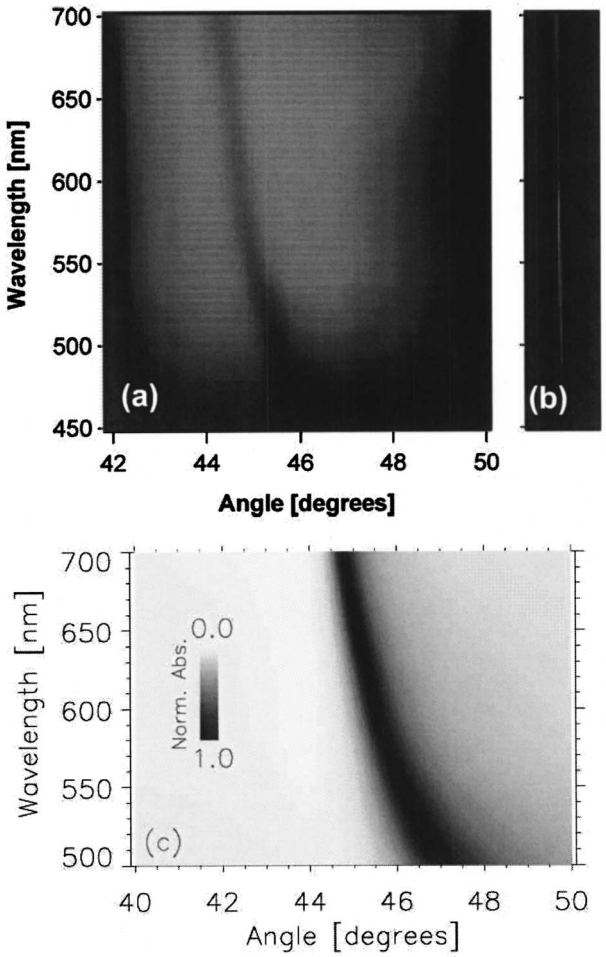

FIG. 3. Comparison between experimental and theoretical SP dispersion relations for silver at room temperature. In (a), we measure the SP dispersion relation in the visible range, where the dark line shows the energy loss of the excitation photons through the SPs. We illustrate in (b) the complementary (roughness induced) scattered light through the thin silver film and give in (c) the simulated SP dispersion relation at room temperature. A good agreement with the experimental measurement is clearly observed. For example, at 700 nm, the measured angle (θ_{exp}) equals 44.4° against a θ_{calc} of 44.7°, at 600 nm, θ_{exp}=44.8° and θ_{calc}=45.0°, and at 500 nm θ_{exp}=45.8° and θ_{calc}=46.8°. The larger difference in the smaller wavelengths may be attributed to the broadening of the absorption.

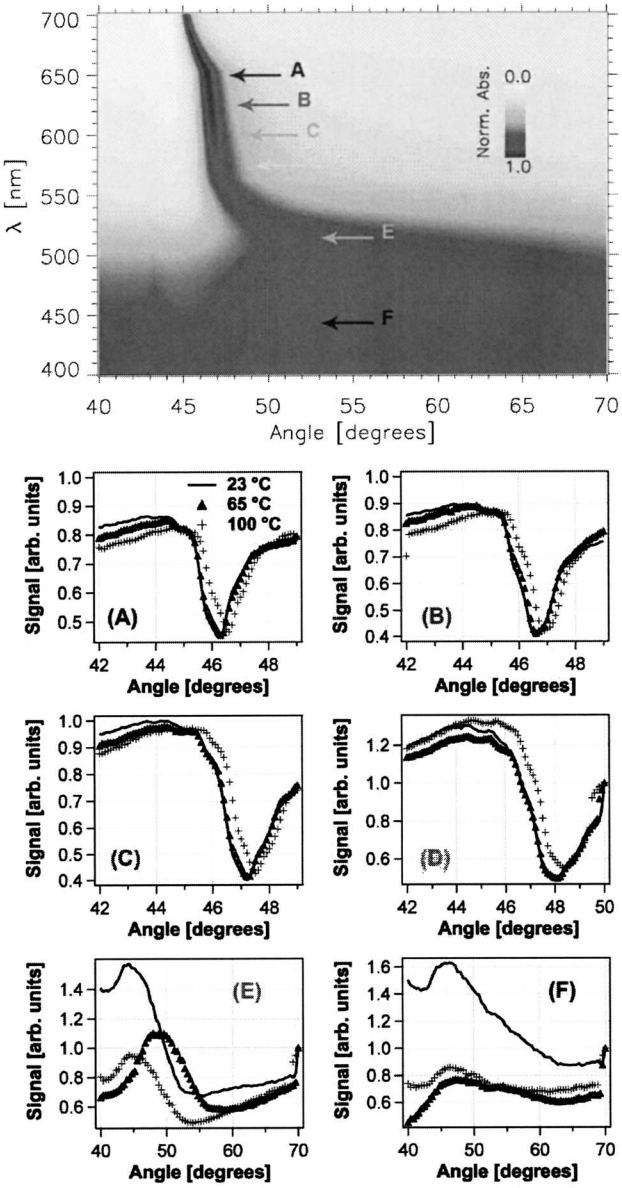

FIG. 4. Absorption curves of a temperature controlled 55 nm gold film, excited at different wavelengths [see Fig. 1(b)]. The top figure shows the simulation of the SP dispersion relation in the entire visible spectrum at room temperature. The continuous curves display the absorption curves at room temperature; the curves, symbolized by (▲) and (+), represent the absorption curves at film temperatures of T_a=65 °C and T_b=100 °C, respectively. The experimentally measured wavelengths go from 650 (A) to 442 nm (F), passing by 625 (B), 600 (C), 575 (D), and 514 nm (E). A good agreement between the simulation and experiment is shown.

carried out for each temperature and wavelength involved. The shift to higher values in the SP resonance angle and the widening of the absorption peak are once more observed, as shown in Fig. 4, and confirm the previous experiments for temperatures below 100 °C. A good agreement with the simulation[22] is also given Fig. 4, where the measured angle (θ_{expt}) equals 46.3° against a calculated angle (θ_{calc}) of 46.4° for 650 nm, at 625 nm, θ_{expt}=46.6° and θ_{calc}=46.7° at 600 nm θ_{exp}=47.2° and θ_{calc}=46.9, and finally at 575 nm, θ_{expt}=48.0° and θ_{calc}=47.2°. For the two examined lower wavelengths, the agreement remains, and no precise angle is observed, as expected for the film thickness and material used.

By treating the real and imaginary parts of the dielectric function of the thin film as parameters, the reflectance can be calculated as a function of the photon wavelength and angle of incidence by solving Maxwell's equation in a two-dimensional domain composed of a semi-infinite dielectric medium (here, quartz with $n=1.46+0\times i$ for the spectral range considered), the metal, and a semi-infinite vacuum or air ($n=1$). By using curve fitting to the function representing the reflectance, this technique allows the extraction of the complex dielectric function from the experimental absorption curves as a function of temperature. A good agreement is found with previous values published by Palik[22] for room

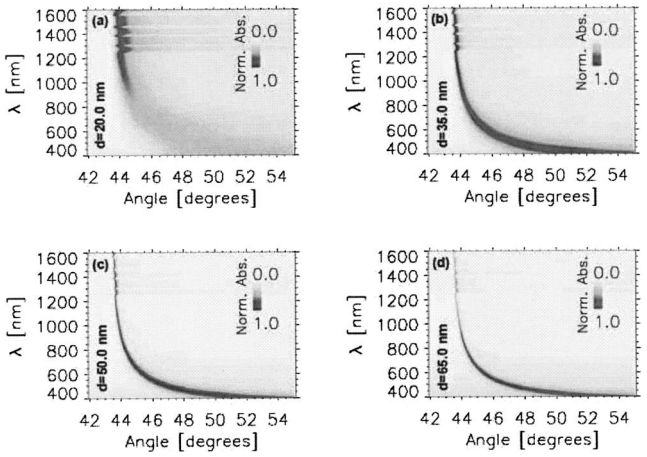

FIG. 5. Computed SP dispersion relation for different silver film thicknesses d. The jaggedness observed for higher wavelengths is due to variations in the reported experimental values for the dielectric function of silver (see Ref. 22).

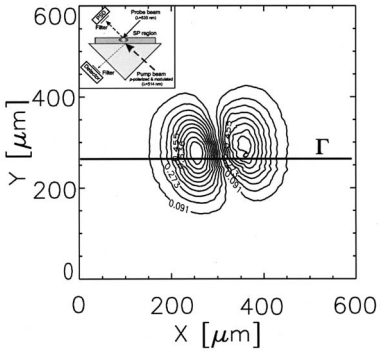

FIG. 6. Normalized contour plot of the surface deformation created by SP excitation in a thin gold film using the Kretschmann configuration (see inset). This plot results from the evaluation of the deflection of the probe laser beam (see inset) locked on the modulation frequency of a 514 nm Ar^+ laser line, while scanning the SP excitation region. The continuous line illustrates the approximate location where further investigation have been carried out (see Fig. 7).

temperature. These results of numerical fittings for the extraction of $n=n(T)=n_r(T)+in_c(T)$ will appear elsewhere. The configuration in Fig. 1(b) allowed us to achieve higher accuracy measurements and to observe more pronounced variations for lower temperatures than those in the first arrangement.

In comparing the results, we also note that while the images of the dispersion relations in Figs. 2 and 3 were for a 40 nm silver film, the measurements at specific wavelengths in Fig. 4 were carried out for a gold film. The variation of the dispersion relation of silver with the film thickness is displayed in Fig. 5. For a thickness of $d=20$ nm [Fig. 5(a)], weak and broad absorptions are seen for lower wavelengths. In Figs. 5(b) and 5(c), d equals 35 and 50 nm, respectively, where absorption exists in the entire considered wavelengths interval; although for 50 nm, the absorption at higher wavelengths is much weaker. For Fig. 5(d), d is taken at 65 nm, and no absorption is observed for higher wavelengths.

III. PROFILING THE DEVICE THERMAL RESPONSE IN THE SP EXCITATION REGION

In this section, we seek to provide qualitative evidence to link the thermal expansion in the excitation region with the heat generated by the nonradiative decay of surface plasmons. The thermal effect may be experimentally examined by profiling the excitation region with an optical beam deflection technique that is highly sensitive to surface height, especially with harmonic displacement using lock-in detection. Similar approaches have been reported to detect deflections as small as 0.03 Å when calibrating a scanning tunneling microscope tip.[23] The resulting surface profiles exhibit a frequency response and a power response, both strong indicators that thermal expansion is the responsible mechanism.

A pump-probe technique, schematically depicted in the inset of Fig. 6, is employed to evaluate surface deformations of the SP excitation region.[18,24] A 1 mW output power, 635 nm wavelength probe laser beam, and a position sensing detector (PSD), aligned and fixed in relation to each other, are scanned as a rigid unit over the top surface of the metal film (deposited on a quartz prism substrate). When the probe beam impinges the metal surface (a 36 nm gold film due to the chosen pump wavelength), the change in the surface height and slope modifies the destination of its deflection, which is discerned by the PSD. We note that slope changes will bring about more deflection than height variations, so that the peripheries of a raised region will be emphasized.[24] The SPs are resonantly excited by a 514 nm line of an Ar^+ laser (incident at an angle of 52° corresponding to a minimum in the reflectance) that is intensity modulated with a mechanical chopper. The diameters of both the pump and the probe beams were below 100 μm (spot size). In the case of the pump beam, the distance between the two center contours in Fig. 6 closely estimates the main beam diameter. By using a metal grading in place of the thin film, the spatial resolution of the probe beam was determined to be ≈ 3 μm.

The resulting harmonic output voltage of the PSD is measured by a lock-in amplifier operating with the chopper frequency as its external reference. The probe is scanned over a 600×600 μm^2 area containing the SP excitation region with a uniform mesh of 3 μm cell size at a constant power of 61 mW and modulation frequency of 200 Hz. A change in film surface height is clearly detected by the optical beam deflection arrangement, as profiled in Fig. 6. Further analysis of the observed effect was performed by line scans (see the continuous line Γ in Fig. 6) across the region at various frequencies and intensities.

The line scans across the center of the SP excitation region were performed at a fixed power of 34 mW and variable chopper frequencies ranging from 50 to 3600 Hz, as shown in Fig. 7(a). The pump laser power at the metal film was measured with a calibrated power meter, by taking into account the 4% loss (by reflection) through the quartz prism. The normalized surface response is the greatest at low frequencies and nonlinearly drops with increasing frequency, which we believe to be due to the thermal relaxation of the

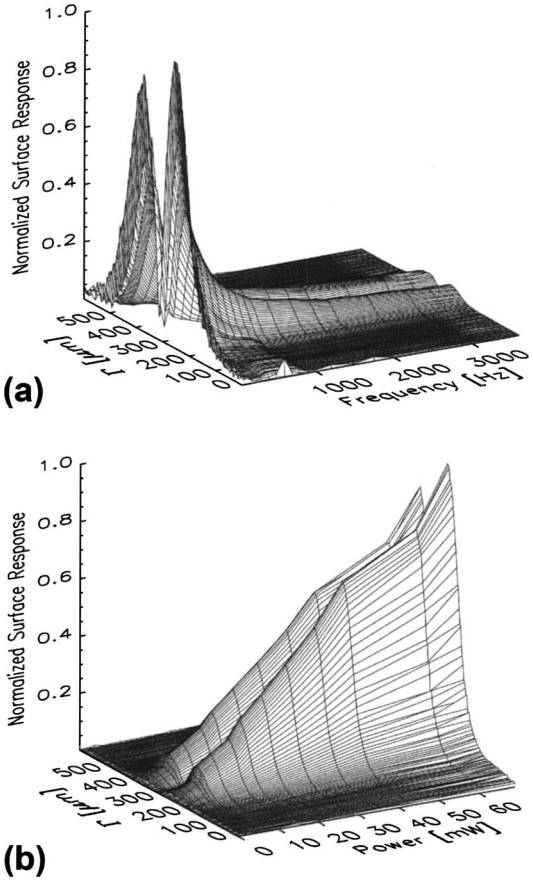

FIG. 7. Experimental measurements of the surface deformation as a function of frequency and incident power. Line scans across the center of the region of SP excitation (along the line Γ, see Fig. 6) at various chopper frequencies in (a) and at fixed frequency and various excitation power levels in (b). In (a), we show a nonlinear response of the surface profile, where a curve following the function $y=a\times x^b$ may be fitted to the normalized maximum response at each frequency measured. In (b), we observe a linear response of the surface profile as a function of power. The normalized maximum response at each power level behaves as a simple function, $y=a+bx$, which describes this linearity. The laser power dependence is an indication of thermal effects such as volumetric expansion.

film-substrate system, as shown in Fig. 7(a). As the frequency increases and the oscillation period becomes closer to the thermal time constant of the metal film, the system cannot react fast enough.[25,26] This frequency dependence is reinforced by investigating the behavior of the normalized maximum response versus frequency. The latter is described by the function $y=a\times x^b$, where y is the response, x is the frequency, $a=12.82\pm1.11$, and $b=-0.64\pm0.02$. The marked drop in thermal response of the gold film near the modulation of 3.5 kHz is in agreement with results reported by Borca-Tasiuc and Chen[26] using a 2 μm laser beam width on a 150 nm gold thin film.

Similar line scans across the same SP excitation region were executed at a fixed chopper frequency of 200 Hz and variable calibrated power levels between 0 to 69 mW, as shown in Fig. 7(b). As expected, increasing local expansion occurs with increasing power intensity. It is shown that a linear behavior is observed at these power levels. The linearity may be described by the function $y=a+bx$, where y is the response, x is the power, $a=-0.006\pm0.007$, and $b=0.0141\pm0.0003$. At increasingly higher power levels, assuming no film damage, we expect the thermal response to eventually taper off, as the gold film–quartz substrate system becomes unable to fully restore to room temperature before the next heating cycle.

In summary, the profiling of the SP excitation region has revealed frequency and power dependence of thermal effects such as the volumetric expansion of the film-substrate system, proffering strong evidence that the decay of SPs is responsible for thermal processes in the metal film that are manifested by thermal expansion, localized heating, and localized thermal gradients.

IV. CONCLUSIONS

By continuing and expanding on our recent work on thermoplasmonic-based modulation, we investigated the influence of thermal effects on the SP dispersion relation. Our experimental work demonstrated an increasing angular shift and broadening in the SP dispersion relation. We employed two different experimental methods to measure the complex index of refraction as the temperature of the surface plasmon supporting film is varied by an external device. The culmination of the experiments cover a temperature range from 23 to 170 °C (Sec. II). We then explore the thermal effects of the thin film due to the optically induced heating scheme furnished by the nonradiative decay of SPs. The profiling of the metal surface with an optical probe revealed surface deformations within the excitation region, which we believe to be due to thermal expansion of the film. The characteristics of frequency and laser power dependent profiles provide evidence that the topographical distortions are due to thermal expansion from thermoplasmonic processes (Sec. III).

In a series of experiments, we have carried out measurements and reported results that have introduced SPs as the active excitation in various photothermal processes. The exploitation of SPs in this manner can have a great impact in well-established as well as emerging SP research, such as SPR sensors or integrated photonic components. The capability of SPs to mediate absorption from a photon field and/or a subsequent source of heat that is generated in individual nanoparticles could also open up possible applications in the field of metamaterials, for example. Moreover, altering the local value of the dielectric function via the thermo-optic coefficient may be of a great interest in the development of microelectronic or photonic components based on thin solid films, such as filters or absorbers. Finally, this investigation may also bring interests in the numerous studies concerning surface plasmon and localized plasmon interactions with molecular entities positioned at the proximity of resonant metallic structures.

ACKNOWLEDGMENTS

This work was supported in part by the SERRI Program of DHS and by the DOE ERSP Program. Oak Ridge National Laboratory in Oak Ridge, Tennessee 37831-6123 is managed by UT-Battelle, LLC for the Department of Energy under

Contract No. DE-AC05-0096OR22725. The authors would like to dedicate this article to the memory of the deceased E. Arakawa for his fruitful discussions and his constant support.

[1]M. Rücker, W. Knoll, and J. P. Rabe, J. Appl. Phys. **72**, 5027 (1992).
[2]S. Grafström, J. Appl. Phys. **91**, 1717 (2002).
[3]J. D. James, J. A. Spittle, S. G. R. Brown, and R. W. Evans, Meas. Sci. Technol. **12**, R1 (2001).
[4]R. H. Ritchie, Phys. Rev. **106**, 874 (1957).
[5]T. L. Ferrell, T. A. Callcott, and R. J. Warmack, Am. Sci. **73**, 344 (1985).
[6]J. M. Brockman, B. P. Nelson, and R. M. Corn, Annu. Rev. Phys. Chem. **51**, 41 (2000).
[7]J. Homola, S. S. Yee, and G. Gauglitz, Sens. Actuators B **54**, 3 (1999).
[8]J. Homola, Anal. Bioanal. Chem. **373**, 528 (2003).
[9]S. Herminghaus and P. Leiderer, Appl. Phys. A: Solids Surf. **51**, 350 (1990).
[10]B. Chadwick and M. Gal, Jpn. J. Appl. Phys., Part 1 **32**, 2717 (1993).
[11]Ş. K. Özdemir and G. Turhan-Sayan, J. Lightwave Technol. **21**, 805 (2003).
[12]H.-P. Chiang, Y.-C. Wang, P. T. Leung, and W. S. Tse, Opt. Commun. **188**, 283 (2001).
[13]H.-P. Chiang, Y.-C. Wang, and P. T. Leung, Thin Solid Films **425**, 135 (2003).
[14]A. Passian, A. L. Lereu, E. T. Arakawa, A. Wig, T. Thundat, and T. L. Ferrell, Opt. Lett. **30**, 41 (2005).
[15]A. L. Lereu, A. Passian, J. P. Goudonnet, T. Thundat, and T. L. Ferrell, Appl. Phys. Lett. **86**, 154101 (2005).
[16]A. Passian, A. L. Lereu, R. H. Ritchie, F. Meriaudeau, T. Thundat, and T. L. Ferrell, Thin Solid Films **497**, 315 (2006).
[17]A. Passian, A. L. Lereu, E. T. Arakawa, R. H. Ritchie, T. Thundat, and T. L. Ferrell, Appl. Phys. Lett. **85**, 2703 (2004).
[18]A. Passian, A. L. Lereu, R. H. Farahi, T. L. Ferrell, and T. Thundat, *Trends in Solid Film Research* (Nova Science, New York, 2007).
[19]E. Kretschmann, Z. Phys. **241**, 313 (1971).
[20]S. C. Kitson, W. L. Barnes, G. W. Bradberry, and J. R. Sambles, J. Appl. Phys. **79**, 7383 (1996).
[21]J. Yoon, G. Lee, S. Ho Song, C.-H. Oh, and P.-S. Kim, J. Appl. Phys. **94**, 123 (2003).
[22]E. D. Palik, *Handbook of Optical Constants of Solids* (Academic, New York, 1985).
[23]G. C. Wetsel, Jr., S. E. McBride, R. J. Warmack, and B. van de Sande, Appl. Phys. Lett. **55**, 528 (1989).
[24]A. Passian, S. Zahrai, A. L. Lereu, R. H. Farahi, T. L. Ferrell, and T. Thundat, Phys. Rev. E **73**, 066311 (2006).
[25]K. Watabe, P. Polynkin, and M. Mansuripur, Appl. Opt. **44**, 3167 (2005).
[26]T. Borca-Tasciuc and G. Chen, Int. J. Thermophys. **19**, 557 (1998).